



Improvements in SO₂ pollution in India: role of technology and environmental regulations

Jayanarayanan Kuttippurath¹ · Vikas Kumar Patel¹ · Mansi Pathak¹ · Ajay Singh^{1,2}

Received: 24 December 2021 / Accepted: 2 June 2022 / Published online: 13 June 2022
© The Author(s), under exclusive licence to Springer-Verlag GmbH Germany, part of Springer Nature 2022

Abstract

India relies heavily on coal-based thermal power plants to meet its energy demands. Sulphur dioxide (SO₂) emitted from these plants and industries is a major air pollutant. Analysis of spatial and temporal changes in SO₂ using accurate and continuous observations is required to formulate mitigation strategies to curb the increasing air pollution in India. Here, we present the temporal changes in SO₂ concentrations over India in the past four decades (1980–2020). Our analysis shows that the Central and East India, and Indo-Gangetic Plain (IGP) are the hotspots of SO₂, as these regions house a cluster of thermal power plants, petroleum refineries, steel manufacturing units, and cement industries. Thermal power plants (51%), and manufacturing and construction industries (29%) are the main sources of anthropogenic SO₂ in India. Its concentration over India is higher in winter (December–February) and lower in pre-monsoon (March–May) seasons. The temporal analyses reveal that SO₂ concentrations in India increased between 1980 and 2010 due to high coal burning and lack of novel technology to contain the emissions during the period. However, SO₂ shows a decreasing trend in recent decade (2010–2020) because of the environmental regulations and implementation of effective control technologies such as the flue gas desulphurisation (FGD) and scrubber. Since 2010, India's renewable energy production has also been increased substantially when India adopted a sustainable development policy. Therefore, the shift in energy production from conventional coal to renewable sources, solid environmental regulation, better inventory, and effective technology would help to curb SO₂ pollution in India. Both economic growth and air pollution control can be performed hand-in-hand by adopting new technology to reduce SO₂ and GHG emissions.

Keywords Sulphur dioxide · India · Sustainable development · Renewable energy · Coal · FGD

Responsible Editor: Gerhard Lammel

Highlights

- Indo-Gangetic Plain and Central India are the hotspots of SO₂ pollution in India.
- Rural population in north and eastern India are exposed to high levels of SO₂.
- Power plants, manufacturing, and construction industries are the major SO₂ sources.
- SO₂ shows decreasing trends since 2010 due to novel technology and regulations.

✉ Jayanarayanan Kuttippurath
jayan@coral.iitkgp.ac.in

¹ CORAL, Indian Institute of Technology Kharagpur, Kharagpur 721302, India

² AgFE Department, Indian Institute of Technology Kharagpur, Kharagpur 721302, India

Introduction

Sulphur dioxide (SO₂) is a part of a chemical group called sulphur oxide, which is a short-lived, colourless, and foul-smelling toxic gas, and is also classified as a “criteria pollutant” by the European Commission in 2015 and the US Environmental Protection Agency in 2016. It is released from refineries, power plants, volcanoes, smelting of metal, and fossil fuel burning (National Ambient Air Quality Status and Trends 2019). High amounts of SO₂ in the atmosphere can degrade air quality and cause acid rain (Tecer and Tagil 2013). Harmful chemical compounds like sulphurous acid (H₂SO₃), sulphuric acid (H₂SO₄), and sulphate aerosol (SO₄²⁻) are formed by the oxidation of SO₂ in the gaseous-phase reactions with the hydroxyl (OH) radical and aqueous-phase reactions with hydrogen peroxide (H₂O₂) or O₃. Sulphate aerosols are also responsible for producing particulate matter (PM) of aerodynamic diameter < 2.5 μm (PM_{2.5}).

These aerosols can impact regional climate by modifying the radiative forcing (Seinfeld and Pandis 2006), and affect cloud reflectivity and precipitation. Apart from these, sulphate aerosols reduce visibility and contribute to acid rain that damages the terrestrial and aquatic ecosystems. It is a precursor for tropospheric ozone, and nitrate and sulphate aerosols (Seinfeld and Pandis 2006).

SO₂ has an adverse effect on the human respiratory system and even short-term exposure to high levels might result in death. As per the WHO air quality guidelines (World Health Organization 2021), the recommended 24 h average SO₂ concentration should not be more than 40 µg/m³ for protecting human health. The National Ambient Air Quality Standard (National Ambient Air Quality Status and Trends 2019) in India limits 24 h average SO₂ concentrations of 50 µg/m³, which should not be exceeded 98% of the time in a year. Additionally, a higher level of SO₂ promotes stomatal opening, which makes excessive loss of water from plants and thus, reduces the quality and quantity of plant yield (Varshney et al. 1979). It reacts with surfaces in the gaseous phase and causes discoloration, as in the case of Taj Mahal (Bergin et al. 2015).

Several changes have been observed over the past decades in the global and regional SO₂ emissions. From 1990 to 2015, global SO₂ emissions have decreased by 31%, although there are regional differences in emissions (Smith et al. 2011; Klimontz et al. 2013; Hoesly et al. 2018). For instance, the highest drop in global SO₂ emissions was found between 1990 and 2000, owing to the 54% reduction in Europe (Vestreng et al. 2007; Maas and Grennfelt 2016) and 21% reduction in North America (Lehmann et al. 2007; Hand et al. 2012). In addition, Europe (40%) and the USA (50%) also showed significant reductions in SO₂ emissions during the period 2000–2015 (Aas et al. 2019). However, East Asia experienced a 32% increase in SO₂ emissions in 1990–2000 and about 70% in 1990–2005, but a reduction in emissions thereafter. India's emissions increased from 4.5 to 15 TgS from 1990 to 2015. Crippa et al. (2016) and Tørseth et al. (2012) observed a similar pattern in SO₂ emissions, where developed countries showed a notable reduction in their emissions, whereas the developing countries continued to emit. However, a significant reduction in SO₂ emissions is observed in developing countries due to the stringent emission controls and reduced use of fossil fuels in recent decade.

Recent studies show significant anthropogenic SO₂ emissions from India, which currently exceed that of China and other countries (Li et al. 2017b, a; Aas et al. 2019). Over the last decade (2010–2017), China reduced 62% of its anthropogenic SO₂ emissions by implementing several control measures, such as the implementation of Flue Gas Desulphurisation (FGD) (Wang et al. 2017; Zheng et al. 2018). There are several studies on emissions and inter-annual variability of

SO₂ over China and other countries (Wang et al. 2018; Jie et al. 2012; Zhang et al. 2012; Leishi et al. 2016; Maji and Sarkar 2020), but there is hardly any study on the long-term trends in SO₂ over India. Furthermore, about 33.5 million people inhabit the regions where SO₂ concentration is very high in India (e.g., IGP and Central India).

In India, coal accounts for 66% of 210 GW of its electricity generation capacity. Emissions from the coal-fired power plants are responsible for a large burden on atmospheric pollution. In 2010–2011, 111 plants with an installed capacity of 121 GW consumed 503 million tons of coal and generated 2100 kt of SO₂ (Guttikunda and Jawahar 2014). Therefore, a dedicated long-term study on SO₂ distribution in India is needed to discuss the regional emission sources and devise a strategy to curb these emissions at the source level.

Here, we examine the long-term changes in SO₂ over India, analyse the sources and factors influencing SO₂ changes, and discuss the role of existing environmental regulations and technology to reduce SO₂ pollution. Furthermore, the socio-economic impact of SO₂ pollution in India is also analysed. We use the ground-based and reanalysis data along with emission inventory for this analysis. This work includes a comprehensive assessment of the effectiveness of novel technology and environmental legislation in reducing SO₂ pollution in India.

Data and methods

MERRA-2, CAMS, and CPCB data

We use the reanalysis data to supplement the ground-based measurements as the latter are station specific and sparse (Roy 2021; Courtial et al. 2022). Therefore, we use the Modern-Era Retrospective analysis for Research and Applications Version 2 (MERRA-2) and Copernicus Atmosphere Monitoring Service (CAMS) data. MERRA-2 is a reanalysis data produced using the Goddard Earth Observing System Model version 5 (GEOS-5) (Gelaro et al. 2017). It is an advanced version of MERRA, with a spatial resolution of 0.5° × 0.625° for the period 1979–2020. To simulate particulates, SO₂, and sulphate, Goddard Global Ozone Chemistry Aerosol Radiation and Transport (GOCART) model is used. Anthropogenic and natural sources are considered for the carbonaceous and sulphate aerosol emissions (Randles et al. 2017). These include volcanic and biomass burning sources derived from satellite observations (Schultz et al. 2008), QuickFire Emission Dataset version 2.4r6 (Darmonov and da Silva 2015), and the Global Fire Emissions Database version 3.1 (Randerson et al. 2013). The assimilation of SO₂ concentration in MERRA-2 is completely unconstrained (Randles et al. 2017). Many studies show that MERRA-2 SO₂ data are in good agreement with that of other datasets (Ukhov et al. 2020; Shikwambana et al. 2020).

In addition to MERRA–2, the total column SO_2 from the CAMS reanalysis (CAMSRA) with a resolution of 80×80 km are also employed (Inness et al. 2015). The biomass burning emissions from the CAMS Global Fire Assimilation System, and anthropogenic and biogenic emissions from the MAC City and MEGAN model, respectively, are used as the input to the CAMS model. It is a three-dimensional model that simulates atmospheric composition, aerosols, dust, carbonaceous aerosol, SO_2 , and other chemical species.

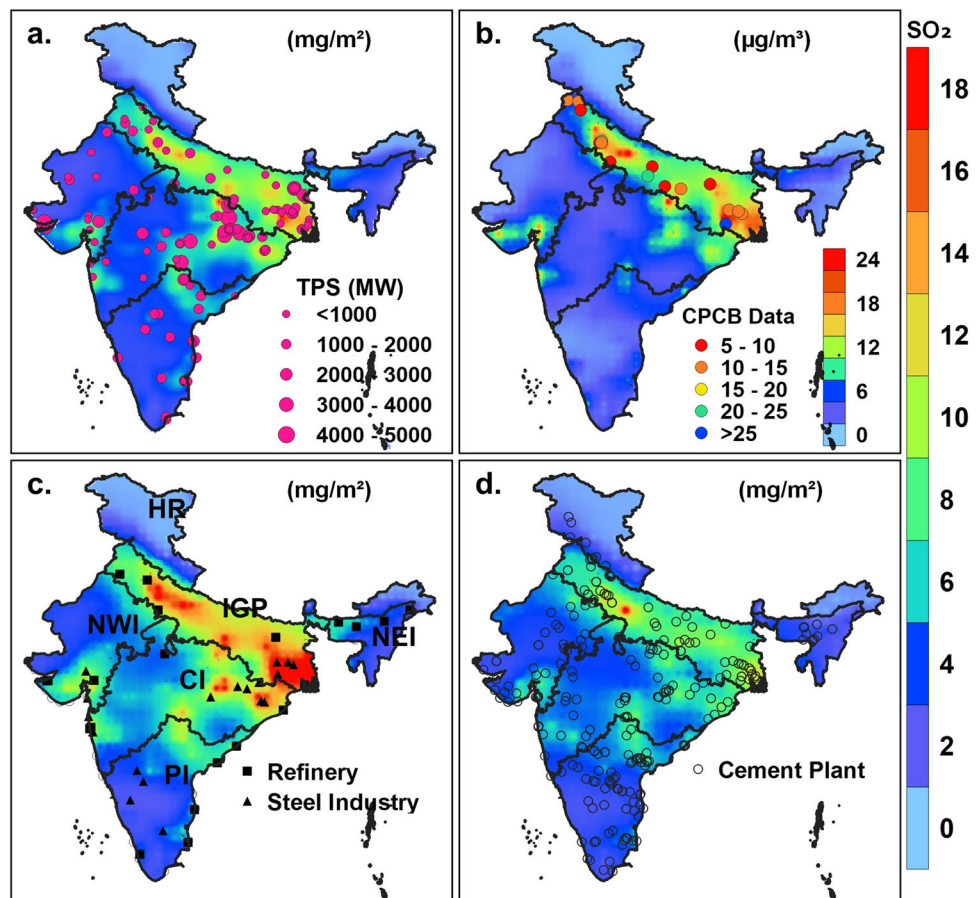
The monthly averaged total column SO_2 data from MERRA–2 (1980–2020) and CAMSRA (2003–2020) are considered to study its seasonal and annual distribution over India. Along with column density, SO_2 mass concentration measurements from twenty surface stations in Indo-Gangetic Plain (IGP) run by the Central Pollution Control Board (CPCB) (Table S1) are also taken for the period 2013–2020. An analysis is also carried out for specific regions in India by finding their spatial average. The regions considered are Central India (CI), North Eastern India (NEI), Peninsular India (PI), northwest India (NWI), IGP, and Hilly Regions (HR), as displayed in Figure 1. Here, the seasons are defined as winter (December, January, and February; DJF), pre-monsoon (March, April, and May; MAM), monsoon (June, July, August, and September; JJAS), and post-monsoon (October

and November; ON). The long-term trends are computed using the linear regression, and the statistical significance is defined with respect to the 95% confidence interval. To investigate the influence of major anthropogenic activities on SO_2 changes, the contribution from coal-based thermal power stations (TPS), steel production units, cement manufacturing industries, sugarcane mills, and refineries are considered.

Inventory data from EDGAR

The Emissions Database for Global Atmospheric Research (EDGAR) is a bottom-up inventory for air pollution and greenhouse gases (Crippa et al. 2018). EDGAR provides emissions as national totals and grid maps at $0.1^\circ \times 0.1^\circ$ resolution, with yearly and monthly data from 1970 to 2015. Here, we use data for the period of 1980–2015 to be consistent with the SO_2 observation period. Energy, industrial operations, product consumption, agriculture, garbage, and other anthropogenic sources are the sectors considered in this inventory. The emission per source and country are calculated using the activity data and emission factors. Major anthropogenic sectors such as thermal power plants, manufacturing and steel industries, transport sector, oil and

Fig. 1 **a** Average annual SO_2 column mass density as analysed from MERRA–2 (1980–2020), overlaid with the location of thermal power plants with their installed capacity over Indian regions. **b** SO_2 surface mass concentration derived from MERRA–2 and CPCB measurements (Circle) from 2013 to 2020. **c** SO_2 column mass density as analysed from MERRA–2 (2003–2020) overlaid with the location of steel and refinery Industries. **d** SO_2 column mass density as analysed from CAMS (2003–2020) overlaid with the location of cement plants. The specific areas marked in the India maps are considered for regional analysis as discussed in the text (e.g. CI is Central India)



refinery industries, and biomass burning are analysed. The temporal evolution of SO₂ emissions from different anthropogenic activities is considered together with the cumulative emissions. The total coal consumption in the country has increased owing to its application in electricity production and other industrial units. Here, we also investigate the temporal evolution of coal, electricity, and petroleum consumption together with India's steel and cement production.

Sulphate, fire count, population density, land class, meteorology, and renewable energy data

The sulphate column mass density data are taken from MERRA-2 for the period 1980–2020. The wind, specific humidity, precipitation, and temperature data are also taken from MERRA-2 for the same period. These data are analysed to study their impact on SO₂ distribution and their role in sulphate formation. To assess the socio-economic impact of SO₂ pollution, population density and land class data based on the 2011 Indian census are taken from the NASA Socioeconomic Data and Applications Centre, and

these data have a spatial resolution of 1 × 1 km. The information regarding renewable energy installed capacity for the period 2014–2020 is acquired from the data source of the Ministry of Renewable Energy, Government of India. We have used the cloud-corrected fire count data with a resolution of 1 km from the MODerate Resolution Imaging Spectrometer (MODIS) Terra and Aqua for the period 2001–2020 to assess the influence of biomass burning on regional SO₂ distribution (Friedl et al. 2002; Singh et al. 2021). Further details about these datasets and their descriptions are given in Table 1.

Results and discussion

Annual average SO₂ over India

Figure 1 shows the annual mean SO₂ column in India averaged for the periods 1980–2020 and 2003–2020. It also depicts the location of one of the major anthropogenic sources of SO₂, the thermal power plants with their installed

Table 1 Measurements and data used in this study. The period of availability, source, and other features are provided

Variables	Spatial resolution	Data source	Time period
SO ₂ column mass density	0.5° × 0.625°	MERRA-2 and CAMS	MERRA-2: 1980–2020, CAMS: 2003–2020
Inventory	0.1° × 0.1°	EDGAR V4.2	1980–2015
Sulphate column density	0.5° × 0.625°	MERRA-2	1980–2020
SO ₂ surface mass concentration	----	CPCB, MERRA-2	2013–2020
Meteorological factors	0.5° × 0.625°	MERRA-2	1980–2020
1. 10 m temperature			
2. 10 m u and v wind			
3. 10 m specific humidity			
4. Precipitation			
Fire counts	1 km	MODIS Terra	2001–2020
Population density	1 km × 1 km	NASA Socio-Economic data	2011 Census
Land class	--	NASA Socio-Economic data	--
Topography	30 m	ASTER	--
Thermal power plant location	--	NTPC, TATA power and respective state ministry	--
Steel plant location	--	Ministry of Steel, Govt of India	--
Cement plant location	--	Cement Information System (CIS), Department for Promotion of Industry And Internal Trade (DPIIT), Government of India, Ministry of Commerce & Industry	--
Refinery	--	Ministry of Petroleum & Natural Gas, Govt. of India	--
Coal consumption	--	Ministry of Petroleum & Natural Gas and Ministry of Coal, Govt. of India	1980–2020
Energy consumption	--	Indiastat	1980–2020
Steel production	--	World steel organisation	1991–2019
Sugarcane production	--	Indiastat	1980–2020
Renewable energy capacity	--	Ministry of Renewable Energy, Govt of India	2014–2020
Petroleum consumption	--	Ministry of Petroleum & Natural Gas, Govt. of India	1980–2020
Cement production	--	Indiastat	1980–2020

capacity. The other prominent sources of SO₂ such as steel, refinery, and cement manufacturing plants are also marked. The MERRA-2 (1980–2020) data show the lowest column of about 0–2 mg/m² in HR, as there are no big Industries and manufacturing units for SO₂ emissions. The regions NEI, PI, and NWI and some areas in CI show slightly higher SO₂ values of about 2–6 mg/m², except for the areas located near the thermal power plants. The industrialised regions show high SO₂ amounts of about 8–12 mg/m². The IGP (6–16 mg/m²) region is highly polluted with SO₂ because of many thermal power plants, coal mines, cement industries, and other source of SO₂ there. Therefore, the lower IGP regions with the major coal mines and thermal plants are the hot-spots of SO₂ in India. The upper IGP region also has high SO₂ of about 8–12 mg/m², which can be due to the emissions from other prominent sources such as cement, steel, and other manufacturing industries (see Fig. 1). Although there are sources of SO₂ in PI, CI, and NWI, the columns are lower than that in IGP, which can be attributed to the dispersion of pollutants by the prevailing winds there. In India, power plants with a capacity > 300 MW contribute to most SO₂ emissions, with 63% coal consumption growth (Lu et al. 2013). The largest thermal power plant in Singrauli, Madhya Pradesh (CI), with a capacity of more than 300 MW, contributes to the high SO₂ values in CI.

The CAMS and MERRA-2 data (Figure 1, bottom panel) show high SO₂ amounts in IGP during the common period of 2003–2020. However, the MERRA-2 data overestimate CAMS, particularly in areas where anthropogenic sources are dominant (IGP and the regions near the industries). This might be due to the difference in emission inventories of both data sets. For instance, CAMS utilises MACcity emission inventory for anthropogenic SO₂ emissions, which is available on a 0.5° × 0.5° grid (Granier et al. 2011), whereas MERRA-2 has the EDGAR 4.2 emission inventory with

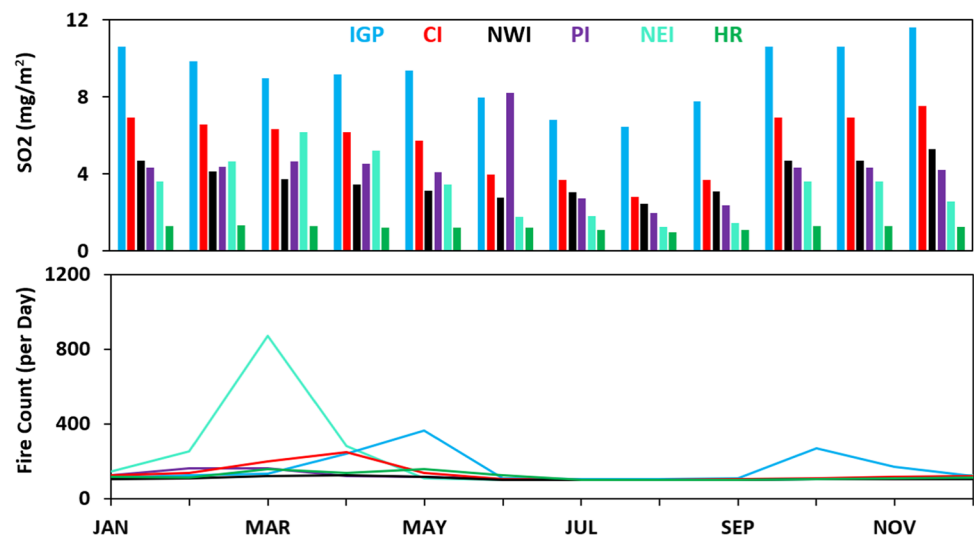
0.1° × 0.1° resolution (Crippa et al. 2018). The spatial resolution of CAMS (80 km) and MERRA-2 (0.5° × 0.625°) and issues in anthropogenic SO₂ simulation are also responsible for the high values in MERRA-2. However, SO₂ data from MERRA-2 are in good agreement with that of CPCB in all cities, although the former shows slightly higher SO₂ in the lower IGP region.

Monthly and seasonal changes

We present the monthly distribution of SO₂ columns over India averaged for the period 1980–2020 using MERRA-2 reanalysis in Fig. S1. The IGP region exhibits a very high amount of SO₂, irrespective of month. The SO₂ concentration decreases from January to March in IGP, but increases in April and May (Fig. 2). Its concentration again decreases in June–July, and the lowest concentration is observed in August. There is a gradual increase in SO₂ concentration from September to December, and the highest concentration is observed during December in IGP. The monthly analyses also reveal that IGP and CI are the hotspots of SO₂ in India, where the concentrations are almost twice that of NEI, NWI, and PI. We also compared the monthly SO₂ total column of MERRA-2 to that of CAMS for the common period of 2003–2020 (Figs. S2, S3). The monthly changes are similar in both data sets, where the differences are due to different periods (i.e. 2003–2020 has a higher concentration than that in 1980–2020 as the SO₂ emission is higher in the former period). As found in the annual averaged SO₂ data, MERRA-2 overestimates CAMS in industrial regions.

Since biomass burning events produce SO₂, we present the fire count analyses for different regions of India between 2001 and 2020, as a proxy for biomass burning (Fig. 2, bottom panel). There are no noticeable fire events in HR, PI, NWI, and CI regions, but a substantial increase

Fig. 2 Top: Monthly SO₂ column mass density over selected Indian regions as analysed from MERRA-2 for the period 1980–2020. Bottom: Panel shows the monthly fire count per day over the same regions for the period 2001–2020



from January (150–200 /day) to March (800–900 /day) is observed over NEI. These fire events are due to the shifting cultivation, which is still practiced in the hilly areas of NEI (Pasha et al. 2020). Shifting cultivation clears the forest through the slash and burn process, and cultivates the crop afterwards. Therefore, SO_2 concentration in NEI increases from January (3 mg/m^2) to March (about 6 mg/m^2), whereas a decrease in SO_2 is observed between January and March in other regions. The IGP region shows two peaks (May and October) in accordance with the Kharif and Rabi harvest seasons, respectively (e.g. Kuttippurath et al. 2020; Singh et al. 2021). Therefore, the biomass or stubble burning contributes to the SO_2 concentrations and both processes affect the annual SO_2 cycle over the regions concerned.

The seasonal distribution of SO_2 averaged over the period 1980–2020 using MERRA–2 observations is shown in Fig. 3. Our analyses reveal that the SO_2 concentration is lowest during the monsoon season. It increases in post-monsoon and reaches its peak in winter. It again decreases during pre-monsoon, and the smallest concentration in the monsoon season is due to the scavenging of SO_2 from precipitation. It is also due to relatively higher humidity during the monsoon season, which helps the formation of sulphate through the oxidation process. However, higher SO_2 amounts of about 10–14 mg/m^2 are observed

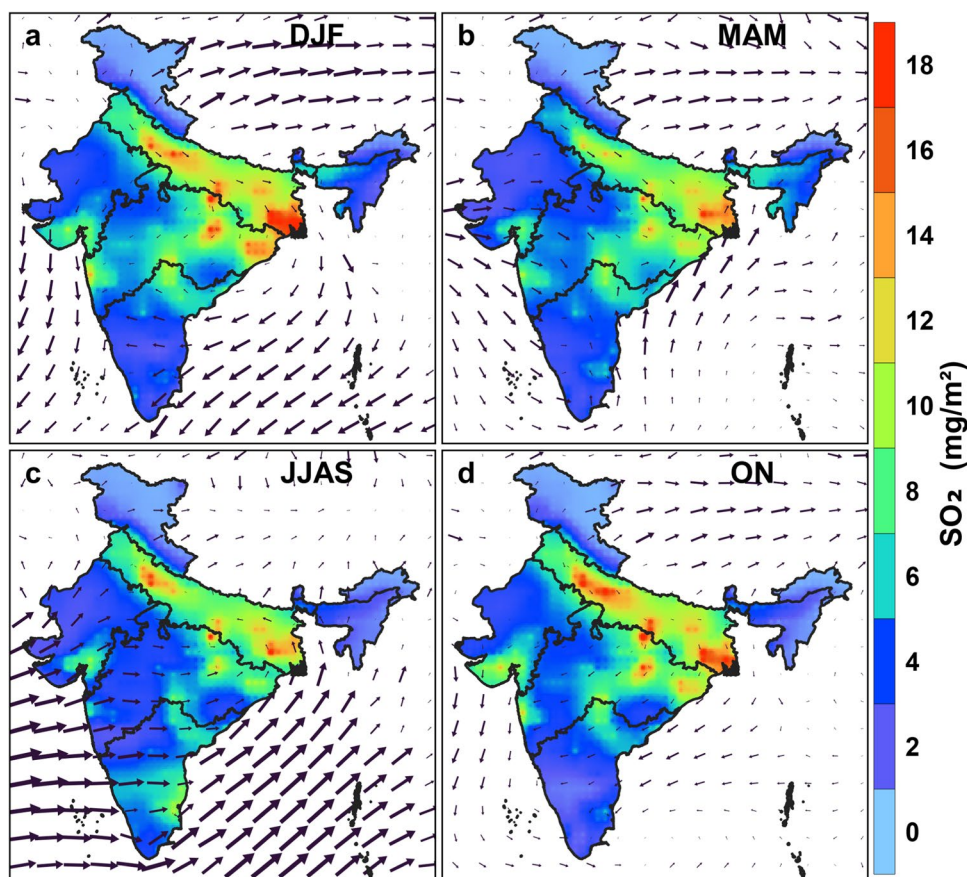
in the industrial areas during the monsoon seasons due to local emitters (i.e. industries in the areas). The sudden rise in SO_2 during post-monsoon can be attributed to the decrease in rainfall in this season. Furthermore, the lower concentration of SO_2 in the pre-monsoon season is associated with the higher temperatures and winds that disperse atmospheric pollutants there.

The highest amount of SO_2 is found during winter because of the lower boundary layer height and low temperature (lower rate of oxidation process) during the season. Additionally, low wind speed restricts the dispersion of pollutants; contributing to the higher SO_2 in winter. The higher SO_2 in regions that are far from the industrial cluster might be due to the winds that transport SO_2 pollutants to these regions. The MERRA–2 data for the common period of 2003–2020 over the same regions show higher values, as shown in Fig. S4. A sudden increase in SO_2 over IGP (12–16 mg/m^2) from 1980–2020 to 2003–2020 in MERRA–2 (8–18 mg/m^2) also reflects the industrial expansion and development in India in recent decades.

Temporal evolution and inventory analysis

Temporal changes in the seasonal SO_2 column from 1980 to 2020 using the MERRA–2 observations reveal a continuous

Fig. 3 Variations of SO_2 column mass density as analysed from MERRA–2 averaged over the period from 1980 to 2020 during (a) winter (DJF), (b) pre-monsoon (MAM), (c) monsoon (JJAS) and (d) post-monsoon (ON) seasons. The overlaid contours are wind vectors



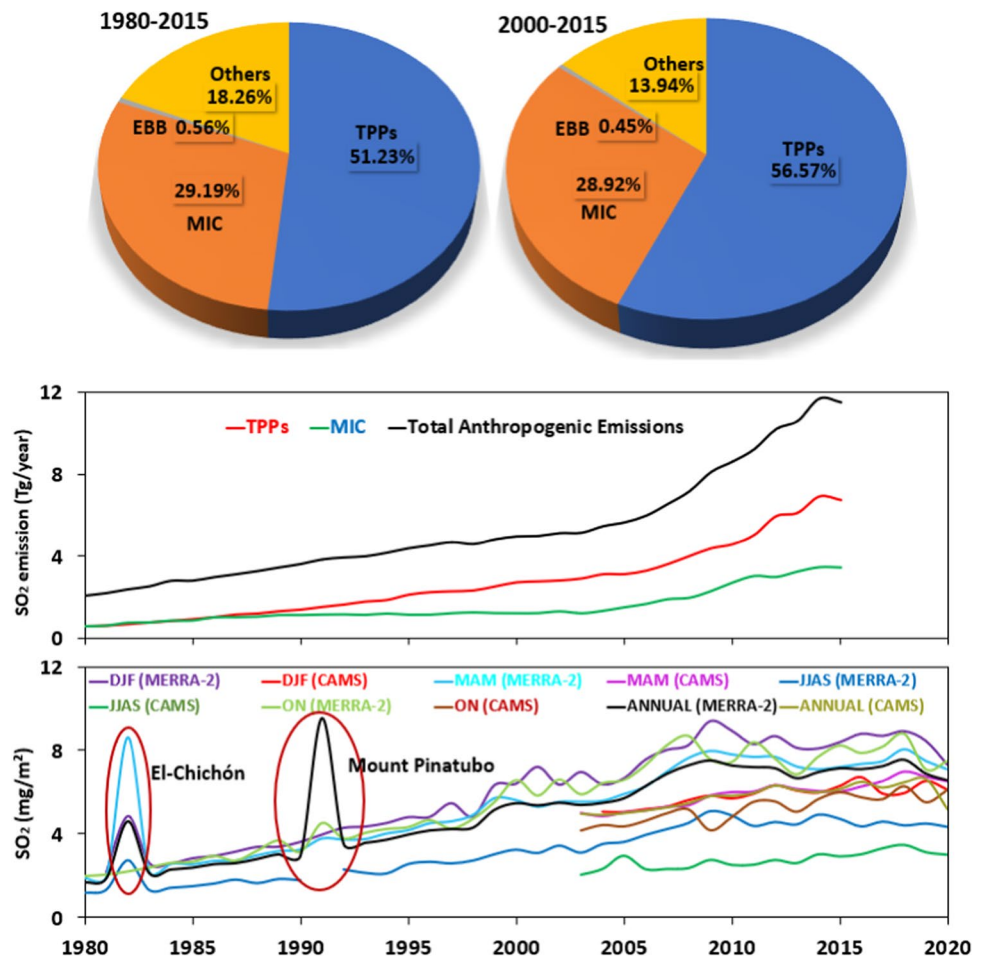
increase in the column until 2010, as demonstrated in Fig. 4. The analysis shows the largest columns in winter, followed by post-monsoon throughout the period. Although CAMS observations in 2003–2020 are not similar, they show comparable results to that of MERRA–2, where the highest SO₂ column is observed in winter and the lowest in monsoon.

The yearly averaged data show similar temporal changes, as the CAMS-derived columns underestimate the MERRA–2 values. The peak observed in 1982 in MERRA–2 is associated with the El Chichon volcanic eruption. The data for the monsoon (June–September) period of 1991 is discarded from the analysis because of the very high values (about 35.3 mg/m²) associated with the Mount Pinatubo volcanic eruption. However, wet deposition of pollutants has reduced the impact of Mount Pinatubo eruption. Soni and Kannan (2003) have also removed the unusually large values from the seasonal analysis and trend detection in their study, and found that the increased turbidity due to the Mt. El-Chichon eruption was smaller than that of Mt. Pinatubo. Together with column SO₂, sulphate concentration also increased substantially during these periods. The seasonality in sulphate concentrations is similar to that of SO₂, as shown in Fig. S5. The energy use in India has increased substantially with coal consumption, as illustrated in Fig. S6. Similarly, the

petroleum consumption, steel, cement, and sugarcane production have also increased in align with the coal consumption, and are the major sources of anthropogenic SO₂ in India (Lu et al. 2011; Sahu et al. 2015). In late 2000, energy consumption and coal burning increased significantly with a higher rate than those in 1980–2000, which made India one of the largest SO₂ emitters in the world (Lu et al. 2011; Li et al. 2017b, a).

Despite the increase in the abovesaid factors, the MERRA–2 data show no increase in SO₂ from 2010 onwards, as shown in Table S3. However, an increase in SO₂ is found in CAMS data in that period, although a record decrease of about 6–8% is observed in 2019 due to the lower coal consumption in that year. A significant reduction in annual mean SO₂ (all India average) in 2020 (about 7–8%) compared to that in recent decade (2010–2020) is also evident due to the national lockdown and accompanied shutdown of industries due to the COVID–19 pandemic. A decrease in SO₂ amount in India during COVID–19 is also reported by other studies (Mahato et al. 2020; Nigam et al. 2021). As demonstrated in Fig. S7, majority of the cities show a constant or decreasing SO₂ concentration from 2013 to 2020. Except for Ranjiganj, which shows a rising trend, the cities near mining sites, such as Dhanbad, exhibit no significant change.

Fig. 4 Temporal evolution of average column SO₂ across the seasons and annual averaged data from 1980 to 2020 in MERRA–2 and 2003–2020 in CAMS. Two major volcanic eruptions are also marked. The very high values during the monsoon season in 1991 (Mount-Pinatubo volcanic eruption) are discarded from the time series. The middle panel illustrates the anthropogenic emissions from thermal power plants (TPPs), manufacturing and construction industries (MIC), and total anthropogenic activities in tera gram (Tg) from 1980 to 2015 using the EDGAR V4.2 inventory. Pie chart (top panel) represents the percentage contributions from TPPs, MIC, EBB (emissions from biomass burning), and others



The near constant SO₂ concentrations since 2010 might be due to the implementation of new environmental laws such as Bharat Stage (BS) II and BS III emission norms in 2005 and 2010, respectively. The stringent emission norms came into force with BS IV in 2017, allowing only 50 ppm of sulphur content in diesel and gasoline. With the implementation of BS VI norms in 2020, only 10 ppm of sulphur content in diesel and gasoline is permitted. The reductions in emissions of SO₂ from other anthropogenic sources, as shown in Fig. S8, also help to contain the SO₂ levels in India. The reduction of SO₂ in 2019 and 2020 provides further evidence that strict environmental regulation, adaptation of better technology, and shift of energy from coal to renewable would help to reduce the air pollution in India. Since 2015, renewable energy production has also increased substantially (Fig. S13) and this would play a vital role in reducing the SO₂ pollution in India. Studies have shown that almost 90% of these SO₂ emissions can be cut by installing FGD at the inlet of the power plant stack (India Brand Equity Foundation [IBEF] 2021). However, the implementation of SO_x and NO_x emission control devices (FGD, scrubber, and selective catalytic reduction) is still slow compared to the electrostatic precipitators for PM_{2.5} control in power plants. As of September 2019, the FGD implementation in the states and private TPSs is about 1% of the proposed FGDs. The Central Electricity Authority plans to implement FGD in 414 TPS units by 2022, which would significantly reduce the overall SO₂ emissions from the power sector (The Energy and Resources Institute [TERI] 2020).

To examine the contributions of different anthropogenic sources of SO₂ in India, an analysis is carried out using the EDGAR-4.2 inventory available for the period 1970–2015. Here, we use the inventory data from 1980 to 2015. The analysis reveals that coal-based thermal power plants are the primary source of SO₂, followed by the manufacturing and construction industries. Emissions from the total anthropogenic activities, including both prominent sources, gradually increased, as shown in Fig. 4 (middle panel). This is because of the gradual increase in electricity demands and industrial production. Thermal power plants alone contributed about 51% of total SO₂ emissions in India from 1980 to 2015, and it increased to 56% in 2000–2015, as shown in Fig. 4 (top panel). Lu et al. (2013) also found that thermal power accounted for 51% of total SO₂ emissions in India in the year 2016. However, the second largest contribution is from the construction and manufacturing industry, with about 29% in 1980–2015. Contributions from other anthropogenic sources are reduced by about 5% in 2000–2015 compared to that in 1980–2015. Furthermore, the contribution to the SO₂ burden over India from biomass burning is less than 1%. Our results are in agreement with that of Li et al. (2017b, a) and Venkataraman et al. (2006), in which they found thermal power plant contribution is much higher than any other sector and the contribution from biomass burning is about 1%.

Emissions from other anthropogenic sources are shown in Fig. S8. The SO₂ emissions from steel or metal industries show a gradual increase, whereas those from railway transport are highly reduced due to its electrification (The Energy and Resources Institute [TERI] 2021). Emissions from other sectors such as civil aviation, chemical industries, and water-born navigation also show a gradual rise, consistent with the increase in transport and industries in recent decades. On the other hand, emission from refineries has decreased significantly from 1995 onwards.

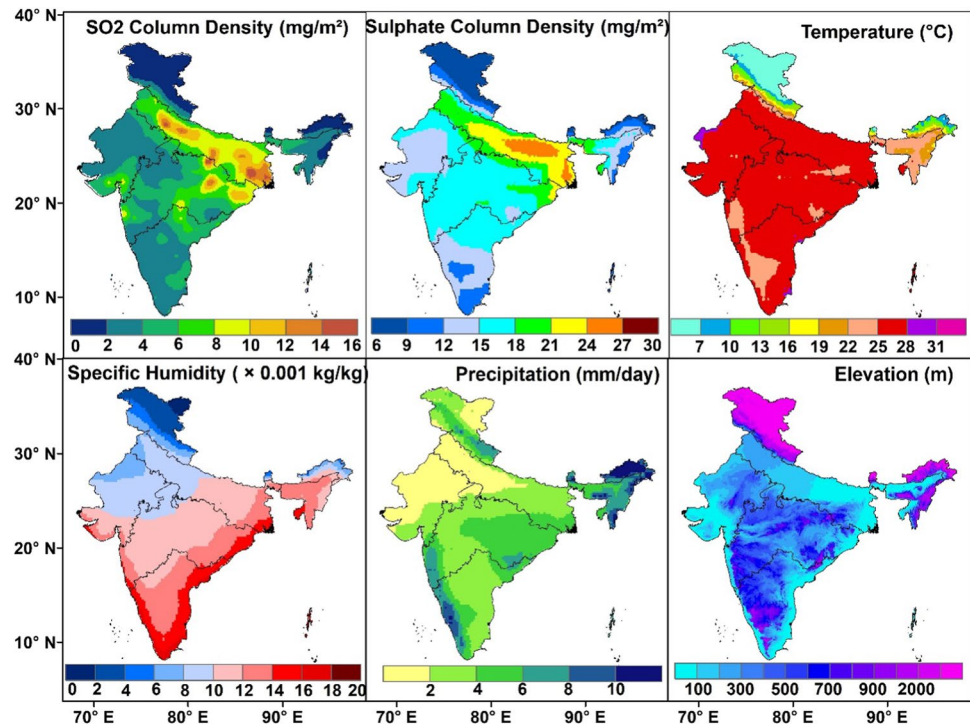
Impact of meteorological factors

Figure 5 shows the annual SO₂ along with sulphate, temperature, specific humidity, precipitation, and topography for the period 1980–2020. Seasonal distribution is shown in Figs. S9–S12. The annual averaged distribution shows very high sulphur (8–12 mg/m²) and sulphate density (21–27 mg/m²) in IGP. Specific humidity and temperature play key roles in converting SO₂ into sulphate (oxidation process). Here, we also observe more sulphate density in the regions where SO₂ concentration is very high, and with higher temperature and specific humidity. Despite higher specific humidity and temperature, relatively lower sulphate amounts are observed in the coastal regions because of lower SO₂ there. Low temperature and high-altitude topography of IGP help to increase SO₂ levels because of the lower boundary layer and poor dispersion of pollutants there, as shown in Fig. S9. The lower column SO₂ in NEI is also due to the wet deposition driven by high precipitation in the region. Higher temperatures are favourable for the dispersion and mixing of pollutants in the atmosphere (Fig. S10). However, higher precipitation in monsoon helps further to reduce SO₂ columns, as demonstrated in Fig. S11, but sulphate is relatively higher during the period due to the high specific humidity and temperature, as this situation enhances sulphate formation. In post-monsoon, higher sulphate concentrations are observed in the upper IGP than that in the lower IGP, albeit with similar temperatures in the region (Fig. S12). This could be due to the comparatively higher precipitation in the lower IGP.

Long-term trends in SO₂

We have estimated the long-term trends in SO₂ over India for different periods: 1980–2020, 1990–2020, 2000–2020, and 2010–2020, as listed in Table S3. The analysis reveals a significant positive trend during 1980–2020 (1.44 mg/m²/dec), 1990–2020 (1.42 mg/m²/dec), and 2000–2020 (0.96 mg/m²/dec) in the annually averaged MERRA-2 data. The seasonal trends are also significantly positive, with a higher rate in winter followed by post-monsoon in all periods, except in 2010–2020. The trends during winter are 1.8 mg/m²/dec in 1980–2020, 1.74 mg/m²/dec in 1990–2020, 1.01 mg/m²/dec in 2000–2020, and –0.45 mg/m²/dec in 2010–2020. The smallest

Fig. 5 Spatial distribution of annual SO₂, sulphate, temperature, specific humidity, and precipitation for the period 1980–2020 from MERRA–2. Elevation topography is shown using the ASTER data



trends in MERRA–2 are computed in monsoon as the SO₂ loading in the atmosphere is very small in this season. Similar results are also estimated from the CAMS data for the period 2000–2020, where positive trends are observed in all seasons and in the annual averaged data. However, negative trends are observed for the period 2010–2020, except in winter. The IGP regions show significantly higher trend values of about 2 mg/m²/dec, as depicted in Fig. 6. Positive trends estimated for PI and HR are comparatively smaller than those estimated for other regions, as the sources of SO₂ are very limited there.

Socio-economic impact of SO₂

India has been in the phase of rapid industrialisation and urbanisation for the past four decades. The process consumed more energy and generated many air pollutants, including SO₂ and GHGs. Currently, India is the third largest producer and second largest consumer of electricity in the world (India Brand Equity Foundation [IBEF] 2021). The country has an installed capacity of 382.15 GW, in which 202.7 GW comes from the coal thermal power generation, 31.6 GW from gas and lignite, and 0.50 GW from the diesel thermal power plants. These constitute 61.5% of the overall installed capacity, as of March 2021 (Central Electricity Authority [CEA] 2021). Energy consumption with industrial development has a significant role in a country's economic growth. Energy, coal and petroleum consumption, and steel and cement production have increased significantly in the past four decades and are a part of the development of India. We have performed a correlation analysis with these factors

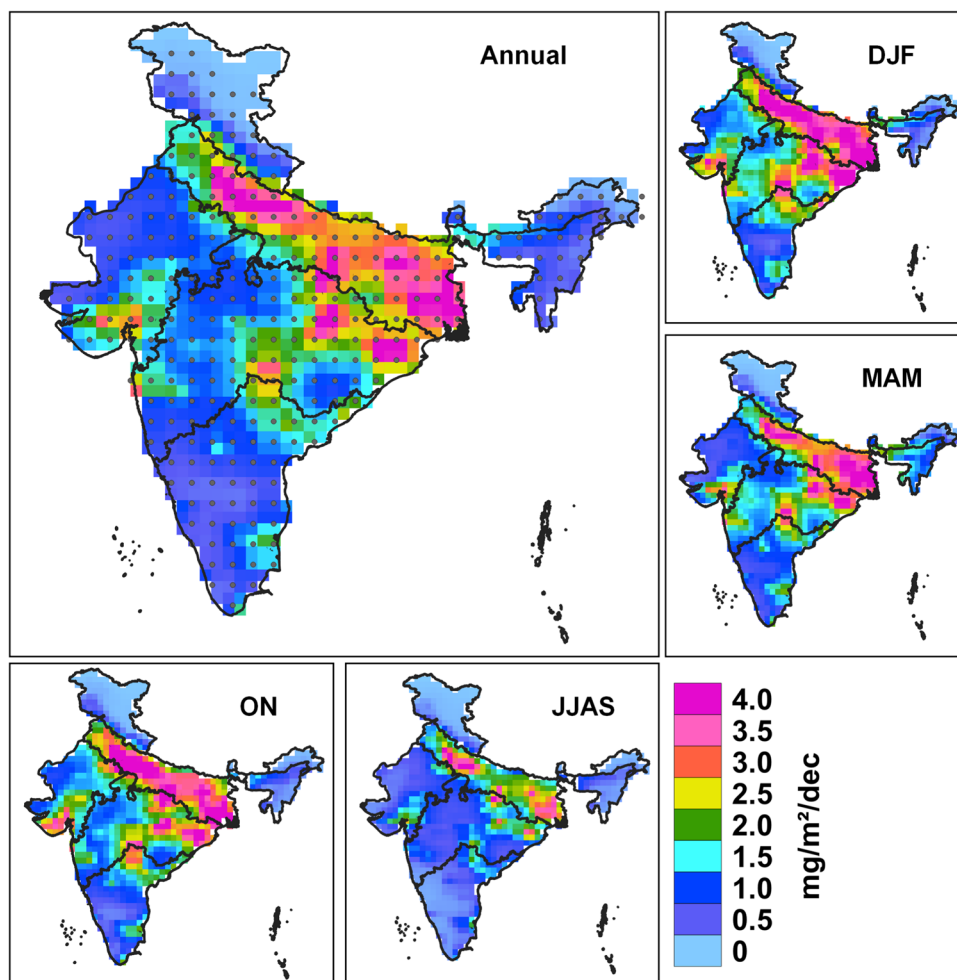
and obtained a high correlation of SO₂ with energy consumption (0.76), steel production (0.87), sugarcane (0.81), cement production (0.98), petroleum (0.80), and coal consumption (0.79) (as shown in Fig. 7 Top panel), suggesting major contribution of these sectors to the increase in SO₂ pollution in India. However, as expected, the correlation with renewable energy is negative (0.5), as it hardly contributes to the pollution. Therefore, an increase in renewable energy production in the future will help to reduce the SO₂ emissions in India.

Our analysis also reveals that the densely populated regions in IGP with high SO₂ pollution include the rural areas, as shown in Fig. 7 (bottom panel). Li et al. (2017b, a) reported that about 33 million people live in regions where SO₂ pollution is high in India. Although SO₂ emission has been constant or decreasing since 2010, it is still higher than that in other countries. India's nationally determined contribution under the Paris Agreement for the period 2021–2030 includes achieving about 40% cumulative electric power installed capacity from non-fossil fuel-based energy resources by 2030 (Ministry of New and Renewable Energy (MNRE) 2020). India is well on its way to achieve these targets and currently has a cumulative installed renewable energy capacity of about 100 GW.

Conclusion and policy implications

We analyse the SO₂ measurements and reanalysis data over India for the period 1980–2020. The SO₂ column shows relatively higher values in winter and autumn in northern

Fig. 6 Annual and seasonal trends for SO₂ column mass density over Indian regions in MERRA–2 from 1980 to 2020. The hatched regions represent the statistical significance at the 95% confidence interval. The trends are statistically significant for all seasons and for the annual averaged data. Therefore, the hatched regions are shown only for the annual averaged trends



India, particularly in IGP and eastern India. The increase in India's energy demands in the past four decades has increased coal consumption, and as a result, more SO₂ is added to the atmosphere during the period. The large capacity thermal power plants in the lower IGP and CI lead to high SO₂ pollution there. Long-term emission inventories need to be constructed for India, particularly for the hotspots for future assessments and policy decisions.

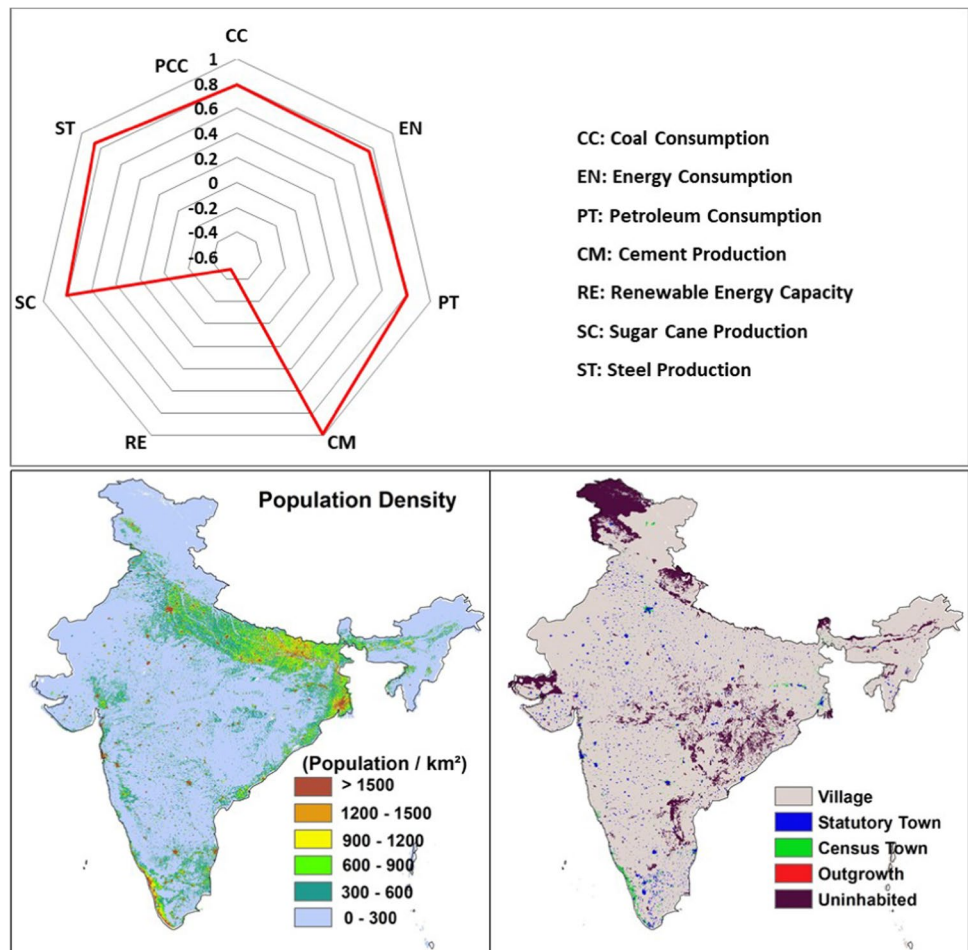
Among the seasons, winter shows the peak in SO₂ due to lower temperature, shallow boundary layer, and reduced wind speed to limit the dispersal of pollutants. A continuous increase in SO₂ emissions is observed from 1980 to 2010, but a reduction in emissions is noted thereafter, as analysed from the MERRA–2 data. This can be due to the strict emission control measures with the implementation of Bharat Stage emission standards (BS) III in 2010, BSIV in 2017, and BSVI in 2020. Replacement of the conventional fuel-based production in the power sector, iron and steel industries, refineries, and other fuel demanding sectors with renewable energy sources would help to reduce the overall SO₂ emissions in India.

Majority of the coal-based thermal power plants in India use bituminous or sub-bituminous coal, or lignite, which

contain 0.7% sulphur by weight. Furthermore, Indian coal (Gondwana coal) contains a lot of ash (35–45%) and has a low calorific value (Reddy and Venkataraman 2002). Therefore, coal-fired power plants should be subjected to pollution standards, similar to those in emerging (such as China) and developed (e.g., EU, Australia, and USA) economies. For example, mandating existing coal-fired power plants to install FGD and scrubber systems can reduce SO₂ pollution.

Due to rapid industrialisation and urbanisation in the past decades, India's energy demand has been increased substantially with coal consumption. Although these help economic development of the country, the air pollution also increases, which is a grave health concern. The analysis shows that the SO₂ emissions in India in the past decade are decreasing (2010–2020) and is an encouraging result. It is achieved primarily due to the strict control measures, adaptation of new technology, and shift towards renewable energy sources during the period. Therefore, both economic growth and air pollution control can be performed hand-in-hand by adopting new technology that helps to reduce SO₂ emissions. These control measures can also

Fig. 7 Population density and land class in India are shown using the NASA socio-economic data based on the 2011 census gridded at $1\text{ km} \times 1\text{ km}$. The top panel shows the Pearson's correlation coefficient between SO_2 column density and energy consumption (EN), steel production (ST), sugarcane production (SC), cement production (CM), petroleum consumption (PT), coal consumption (CC), and renewable energy installed capacity (RE)



mitigate climate change, which is an added advantage of cutting the SO_2 emissions.

We also need an improved air quality monitoring network to understand the spatial and temporal changes of pollutants, which would help to make policies relevant to improve air quality and to meet targeted reduction in emissions. We have not computed the absolute emissions here, and the measurements also have uncertainties. However, the trends computed are statistically significant across all Indian regions. Therefore, our findings have important implications for future environmental policies on India's SO_2 emissions and for understanding the impact of SO_2 on regional climate, air quality, ecosystem dynamics, and public health. This study also provides a baseline for future studies that would critically examine changes in SO_2 pollution as a result of the country's socio-economic development.

Supplementary Information The online version contains supplementary material available at <https://doi.org/10.1007/s11356-022-21319-2>.

Acknowledgements We thank the Director, Indian Institute of Technology Kharagpur (IIT Kgp), Chairman CORAL, IIT Kgp, and the Ministry of Education (MoE) for facilitating the study. VKP, MP, and

AS acknowledge the support from MoE and IIT KGP. We thank Giovanni's online data system developed and maintained by the NASA GES DISC for MERRA-2 data and the MODIS terra team for fire count data. We also acknowledge Copernicus Atmospheric Data Store for CAMS reanalysis data, along with NASA socio-economic portal for population density and land class data. We also thank the respective ministry of Government of India, such as Ministry of Renewable energy, Ministry of coal, Ministry of Steel, Ministry of Petroleum and Natural Gas, Ministry of Commerce and Industry, and Department for Promotion of Industry and Internal Trade (DPIIT) for different datasets. We also thank Indiastat for energy consumption, sugarcane and cement production data, and the world steel organisation for steel production data. We also thank CPCB for surface concentration data.

Author contribution JK: conceptualisation, methodology, data analysis, supervision, visualisation, writing—original draft, review and editing of the original draft; VKP: methodology, data analysis, visualisation, writing—original draft; AS: formal analysis, writing—original draft; MP: formal analysis, writing—original draft.

Data availability The CAMS data: <https://ads.atmosphere.copernicus.eu/#/search?text=reanalysis>. MERRA-2 data: <https://giovanni.gsfc.nasa.gov/giovanni/>. EDGAR V4.2 inventory data: <https://edgar.jrc.ec.europa.eu/>. Cement, sugarcane, and energy consumptions data: <https://www.indiastat.com/Home/DataSearch?Keyword=cement%20producti%20in%20india>. NASA socio-economic data for population density and land class: <https://sedac.ciesin.columbia.edu/data/set/india-spati>

al-india-census-2011/metadata. MODIS fire count data: https://firms.modaps.eosdis.nasa.gov/active_fire/. Location of cement plant: <https://eaindstry.nic.in/cement/report2.asp>. Renewable energy data (MNRE annual report 2020): https://mnre.gov.in/img/documents/uploads/file_f-1618564141288.pdf. Steel production data: <https://www.worldsteel.org/steel-by-topic/statistics.html>.

Declarations

Ethics approval and consent to participate Not applicable

Consent to participate Not applicable.

Consent for publication Not applicable.

Competing interests The authors declare no competing interests.

References

- Aas W, Mortier A, Bowersox V, Cherian R, Faluvegi G, Fagerli H, Hand J, Klimont Z, Galy-Lacaux C, Lehmann CMB, Myhre CL, Myhre G, Olivie D, Sato K, Quaas J, Rao PSP, Schulz M, Sindell D, Skeie RB, Stein A, Takemura T, Tsyro S, Vet R, Xu X (2019) Global and regional trends of atmospheric sulphur. *Sci Rep* 9:1–11. <https://doi.org/10.1038/s41598-018-37304-0>
- Bergin MH, Tripathi SN, Jai Devi J, Gupta T, McKenzie M, Rana KS, Shafer MM, Villalobos AM, Schauer JJ (2015) The discoloration of the Taj Mahal due to particulate carbon and dust deposition. *Environ Sci Tech* 49:808–812
- Central Electricity Authority (CEA) (2021) Installed capacity report. https://cea.nic.in/wp-content/uploads/installed/2021/03/installed_capacity.pdf. Accessed 21 Aug 2021
- Crippa M, Guizzardi D, Muntean M, Schaaf E, Dentener F, van Aardenne JA, Monni S, Doering U, Olivier JGJ, Pagliari V, Janssens-Maenhout G (2018) Gridded emissions of air pollutants for the period 1970–2012 within EDGAR v4.3.2. *Earth Syst Sci Data* 10:1987–2013. <https://doi.org/10.5194/essd-10-1987-2018>
- Crippa M, Janssens-Maenhout G, Dentener F, Guizzardi D, Sindelarova K, Muntean M, Dingenes RV, Granier C (2016) Forty years of improvements in European air quality: regional policy-industry interactions with global impacts. *Atmos Chem Phys* 16:3825–3841. <https://doi.org/10.5194/acp-16-3825-2016>
- Courtial A, Touya G, Zhang X (2022) Constraint-based evaluation of map images generalized by deep learning. *J geovis spat anal* 6:13. <https://doi.org/10.1007/s41651-022-00104-2>
- Darmenov A, da Silva A (2015) The Quick Fire Emissions Dataset (QFED): documentation of versions 2.1, 2.2 and 2.4. Technical Report Series on Global Modeling and Data Assimilation 32: NASA Tech Rep NASA/TM–2015–104606
- Friedl MA, McIver DK, Hodges JCF, Zhang XY, Muchoney D, Strahler AH, Woodcock CE, Gopal S, Schneider A, Cooper A, Caccini A, Gao F, Schaaf C (2002) Global land cover mapping from MODIS: algorithms and early results. *Remote Sens Environ* 83:287–302. [https://doi.org/10.1016/S0034-4257\(02\)00078-0](https://doi.org/10.1016/S0034-4257(02)00078-0)
- Gelaro R, McCarty W, Sourez MJ, Todling R, Molod A, Takacs L, Randles CA, Darmenov A, Bosilovich MG, Reichle R, Wargan K, Coy L, Cullather R, Draper C, Akella S, Buchard V, Conaty A, da Silva AM, Gu W, Kim GK, Koster R, Lucchesi R, Merkova D, Nielsen JE, Partyka G, Pawson S, Putman W, Rienecker M, Schubert SD, Sienkiewicz M, Zhao B (2017) The Modern-Era Retrospective Analysis for Research and Applications, version 2 (MERRA-2). *J Clim* 30:5419–5454. <https://doi.org/10.1175/JCLI-D-16-0758.1>
- Granier C, Bessagnet B, Bond T, D'Angiola A, van Der Gon HD, Frost GJ, Heil A, Kaiser JW, Kinne S, Klimont Z, Kloster S, Lamarque JF, Lioussé C, Masui T, Meleux F, Mieville A, Ohara T, Raut JC, Riahi K, Schultz MG, Smith SJ, Thompson A, van Aardenne J, van der Werf GR, van Vuuren DP (2011) Evolution of anthropogenic and biomass burning emissions of air pollutants at global and regional scales during the 1980–2010 period. *Clim Change* 109:163. <https://doi.org/10.1007/s10584-011-0154-1>
- Guttikunda SK, Jawahar P (2014) Atmospheric emissions and pollution from the coal-fired thermal power plants in India. *Atmos Environ* 92:449–460. <https://doi.org/10.1016/j.atmosenv.2014.04.057>
- Hand JL, Schichtel BA, Malm WC, Pitchford ML (2012) Particulate sulfate ion concentration and SO₂ emission trends in the United States from the early 1990s through 2010. *Atmos Chem Phys* 12:10353–10365. <https://doi.org/10.5194/acp-12-10353-2012>
- Hoesly RM, Smith SJ, Feng L, Klimont Z, Janssens-Maenhout G, Pitkanen T, Seibert JJ, Vu L, Andres RJ, Bolt RM, Bond TC, Dawidowski L, Kholod N, Kurokawa J, Li M, Liu L, Lu Z, Moura MCP, O'Rourke PR, Zhang Q (2018) Historical (1750–2014) anthropogenic emissions of reactive gases and aerosols from the Community Emissions Data System (CEDS). *Geosci Model Dev* 11:369–408. <https://doi.org/10.5194/gmd-11-369-2018>
- India Brand Equity Foundation (IBEF) (2021) Indian power industry report January 2021. Details available at: <https://www.ibef.org/download/Power-January-2021.pdf>. Access 29 Aug 2021
- Inness A, Blechschmidt AM, Bouarar I, Chabrilat S, Crepulja M, Engelen RJ, Eskes H, Flemming J, Gaudel A, Hendrick F, Huijnen V, Jones L, Kapsomenakis J, Katragkou E, Keppens A, Langerock B, de Mazière M, Melas D, Parrington M, Peuch VH, Razinger M, Richter A, Schultz MG, Suttie M, Thouret V, Vrekoussis M, Wagner A, Zerefoset C (2015) Data assimilation of satellite-retrieved ozone, carbon monoxide and nitrogen dioxide with ECMWF's Composition-IFS. *Atmos Chem Phys* 15:5275–5303
- Jie J, Yong Z, Jay G, Jianjun J (2012) Monitoring of SO₂ column concentration change over China from Aura OMI data. *Int J Remote Sens* 33:1934–1942
- Klimontz Z, Smith SJ, Cofala J (2013) The last decade of global anthropogenic sulfur dioxide: 2000–2011 emissions. *Environ Res Lett* 8:014003
- Kuttippurath J, Singh A, Dash SP, Mallick N, Clerbaux C, Van Damme M, Clarisse L, Coheur PF, Raj, S, Abhishek K, Varikoden H (2020) Record high levels of atmospheric ammonia over India: spatial and temporal analyses. *Sci Total Environ* 740. <https://doi.org/10.1016/j.scitotenv.2020.139986>
- Leishi Z, Sheng LC, Ruiqin Z, Liangfu C (2016) Spatial and temporal evaluation of long-term trend (2005–2014) of OMI retrieved NO₂ and SO₂ concentrations in Henan Province, China. *Atmos Environ* 154:151–166
- Li C, McLinden C, Fioletov V, Krotkov N, Carn S, Joiner J, Streets D, He H, Ren X, Li Z, Dickerson RR (2017) India is overtaking China as the world's largest emitter of anthropogenic sulfur dioxide. *Sci rep* 7:1–7
- Li M, Liu H, Geng G, Hong C, Liu F, Song Y, Tong D, Zheng B, Cui H, Man H, Zhang Q, He K (2017) Anthropogenic emission inventories in China: a review. *Natl Sci Rev* 4:834–866
- Lu Z, Streets DG, De Foy B, Krotkov NA (2013) Ozone monitoring instrument observations of interannual increases in SO₂ emissions from Indian coal-fired power plants during 2005–2012. *Environ Sci Technol* 47:13993–14000. <https://doi.org/10.1021/es4039648>
- Lehmann CMB, Bowersox VC, Larson RS, Larson SM (2007) Monitoring long-term trends in sulfate and ammonium in US precipitation: results from the National Atmospheric Deposition Program/National Trends Network. *Water, Air, Soil Pollution. Focus* 7:59–66. <https://doi.org/10.1007/s11267-006-9100-z>
- Lu Z, Zhang Q, Streets DG (2011) Sulfur dioxide and primary carbonaceous aerosol emissions in China and India, 1996–2010.

- Atmos Chem Phys 11:9839–9864. <https://doi.org/10.5194/acp-11-9839-2011>
- Maas R, Grennfelt PE (2016) Towards cleaner air. scientific assessment report 2016, EMEP steering body and working group on effects of the convention on long-range transboundary air pollution. https://www.unece.org/fileadmin/DAM/env/lrtap/ExecutiveBody/35th_session/CLRTAP_Scientific_Assessment_Report_-_Final_20-5-2016.pdf. Accessed 11 Sept 2021
- Mahato S, Pal S, Ghosh KG (2020) Effect of lockdown amid COVID-19 pandemic on air quality of the megacity Delhi, India. *Sci Total Environ* 730:139086. <https://doi.org/10.1016/j.scitotenv.2020.139086>
- Maji KJ, Sarkar C (2020) Spatio-temporal variations and trends of major air pollutants in China during 2015–2018. *Environ Sci Pollut Res* 27:33792–33808. <https://doi.org/10.1007/s11356-020-09646-8>
- Ministry of New and Renewable Energy (MNRE) (2020) Government of India. Annual report on renewable energy (2020–2021). https://mnre.gov.in/img/documents/uploads/file_f-1618564141288.pdf. Accessed 8 Sept 2021
- National Ambient Air Quality Status and Trends (2019) Central Pollution Control Board, Ministry of Environment, Forest and Climate Change, Government of India. https://cpcb.nic.in/upload/NAAQS_2019.pdf. Accessed 17 Aug 2021
- Nigam R, Pandya K, Luis AJ, Sengupta R, Kotha M (2021) Positive effects of COVID-19 lockdown on air quality of industrial cities (Ankleshwar and Vapi) of Western India. *Sci Rep* 11:4285. <https://doi.org/10.1038/s41598-021-83393-9>
- Pasha SV, Behera MD, Mahawar SK, Barik SK, Joshi SR (2020) Assessment of shifting cultivation fallows in Northeastern India using Landsat imageries. *Trop Ecol* 61:65–75. <https://doi.org/10.1007/s42965-020-00062-0>
- Randerson JT, van der Werf GR, Giglio L, Collatz GJ, Kasibhatla PS (2013) Global Fire Emissions Database, Version 3.1 (Version 3). ORNL Distributed Active Archive Center. <https://doi.org/10.3334/ORNLDAAAC/1191>
- Randles CA, da Silva AM, Buchard V, Colaro PR, Darmenov A, Govindaraju R, Smirnov A, Holben B, Ferrare R, Hair J, Shinzuka Y, Flynn CJ (2017) The MERRA–2 aerosol reanalysis, 1980 onward. Part I: System description and data assimilation evaluation. *J Clim*. <https://doi.org/10.1175/JCLI-D-16-0609.1>
- Reddy MS, Venkataraman C (2002) Inventory of aerosol and sulphur dioxide emissions from India: I-fossil fuel combustion. *Atmos Environ* 36:677–697
- Roy A (2021) Atmospheric pollution retrieval using path radiance derived from remote sensing data. *J Geovis Spat Anal* 5:26. <https://doi.org/10.1007/s41651-021-00093-8>
- Sahu SK, Ohara T, Beig G, Kurokawa J, Nagashima T (2015) Rising critical emission of air pollutants from renewable biomass based cogeneration from the sugar industry in India. *Environ Res Lett* 10:095002. <https://doi.org/10.1088/1748-9326/10/9/095002>
- Schultz MG, Heil A, Hoelzemann JJ, Spessa A, Thonicke K, Goldammer JG, Held AC, Pereira JMC, van het Bolscher M (2008) Global wildland fire emissions from 1960 to 2000. *Glob Biogeochem Cycles* 22:GB2002. <https://doi.org/10.1029/2007GB003031>
- Seinfeld JH, Pandis SN (2006) Atmospheric chemistry and physics — from air pollution to climate change (2nd Ed.). John Wiley and Sons, Inc., Hoboken, New Jersey
- Shikwambana L, Mhangara P, Mbatha N (2020) Trend analysis and first-time observations of sulphur dioxide and nitrogen dioxide in South Africa using TROPOMI/Sentinel-5 P data. *Int J Applied Earth Obs Geoinfo* 91:1569–8432. <https://doi.org/10.1016/j.jag.2020.102130>
- Singh A, Kuttippurath J, Abhishek K, Mallick N, Raj S, Chander G, Dixit S (2021) Biogenic link to the recent increase in atmospheric methane over India. *J Environ Manage*. <https://doi.org/10.1016/j.jenvman.2021.112526>
- Smith SJ, van Aardenne J, Klimont Z, Andres RJ, Volke A, Arias SD (2011) Anthropogenic sulfur dioxide emissions: 1850–2005. *Atmos Chem Phys* 11:1101–1116. <https://doi.org/10.5194/acp-11-1101-2011>
- Soni V, Kannan PS (2003) Temporal variations and the effect of volcanic eruptions on atmospheric turbidity over India. *Mausam* 54:881–890
- Tecer LH, Tagil S (2013) Spatial-temporal variations of sulphur dioxide concentration, source, and probability assessment using a GIS-based geostatistical approach, Polish. *J Environ Stud* 22:1491–1498
- The Energy and Resources Institute (TERI) (2020) Emissions control in thermal power stations: issues, challenges, and the way forward. <https://www.teriin.org/sites/default/files/2020-02/emissions-control-thermal-power.pdf>. Accessed 3 Oct 2021
- The Energy and Resources Institute (TERI) (2021) Decarbonization of transport sector in India: present status and future pathways. https://www.teriin.org/sites/default/files/files/Decarbonization_of_Transport%20Sector_in_India.pdf. Accessed 15 May 2022
- Tørseth K, Aas W, Breivik K, Fjaerra AM, Fiebig M, Hjellbrekke AG, Myhre CL, Solberg S, Yttri KE (2012) Introduction to the European Monitoring and Evaluation Programme (EMEP) and observed atmospheric composition change during 1972–2009. *Atmos Chem and Phys* 12:5447–5481. <https://doi.org/10.5194/acp-12-5447-2012>
- Ukhov A, Mostamandi S, Krotkov N, Flemming J, da Silva A, Fioletov V, McLinden C, Anisimov A, Alshehri YM, Stenchikov G (2020) Study of SO₂ pollution in the Middle East using MERRA–2, CAMS data assimilation products, and high-resolution WRF-Chem Simulations. *J Geophys Res* 125(6):e2019JD031993. <https://doi.org/10.1029/2019jd031993>
- Varshney CK, Garg JK, Lauenroth WK, Heitschmidt RK (1979) Plant responses to sulfur dioxide pollution. *CRC Crit Rev Environ Control* 9:27–49. <https://doi.org/10.1080/10643387909381667>
- Venkataraman C, Habib G, Kadamba D, Shrivastava M, Leon JF, Crouzille B, Boucher O, Streets DG (2006) Emissions from open biomass burning in India: Integrating the inventory approach with high-resolution Moderate Resolution Imaging Spectroradiometer (MODIS) active-fire and land cover data. *Glob Biogeochem Cycles* 20. <https://doi.org/10.1029/2005GB002547>
- Vestreng V, Myhre G, Fagerli H, Reis S, Tarrasón L (2007) Twenty-five years of continuous sulphur dioxide emission reduction in Europe. *Atmos Chem Phys* 7:3663–3681. <https://doi.org/10.5194/acp-7-3663-2007>
- Wang J, Zhao B, Wang S, Yang F, Xing J, Morawska L, Ding A, Kulmala M, Kerminen VM, Kujansuu J, Wang Z, Ding D, Zhang X, Wang H, Tian M, Petaja T, Jiang J, Hao J (2017) Particulate matter pollution over China and the effects of control policies. *Sci Total Environ* 584–585. <https://doi.org/10.1016/j.scitotenv.2017.01.027>
- Wang T, Wang P, Theys N, Tong D, Hendrick F, Zhang Q, Van Roozendael M (2018) Spatial and temporal changes in SO₂ regimes over China in the recent decade and the driving mechanism. *Atmos Chem Phys* 18:18063–18078. <https://doi.org/10.5194/acp-18-18063-2018>
- World Health Organization (WHO) (2021) WHO global air quality guidelines: particulate matter (PM_{2.5} and PM₁₀), ozone, nitrogen dioxide, sulfur dioxide and carbon monoxide. World Health Organization, Copenhagen and Geneva. <https://apps.who.int/iris/handle/10665/345329>
- Zhang Q, He K, Huo H (2012) Cleaning China's air. *Nature* 484:161
- Zheng B, Tong D, Li M, Liu F, Hong C, Geng G, Li H, Li X, Peng L, Qi J, Yan L, Zhang Y, Zhao H, Zheng Y, He K, Zhang Q (2018) Trends in China's anthropogenic emissions since 2010 as the consequence of clean air actions. *Atmos Chem Phys* 18:14095–14111. <https://doi.org/10.5194/acp-18-14095-2018>

Publisher's note Springer Nature remains neutral with regard to jurisdictional claims in published maps and institutional affiliations.